DOI: 10.1002/ejic.200900011

A Quantum Chemical Study of the Structure, Bonding Characteristics and Nonlinear Optical Properties of Aryloxido and Salicylaldehydo Derivatives of $[XW_5O_{18}]^{3-}$ (X = Zr or Ti)

Jia Zhuang,[a] Likai Yan,[a] Chunguang Liu,[a] and Zhongmin Su*[a]

Keywords: Polyoxometalates / Organic-inorganic hybrid composites / Natural bond analysis / Nonlinear optics / Density functional calculations

The bonding characteristics, first hyperpolarizabilities, and origin of the nonlinear optical (NLO) properties of aryloxido and salicylaldehydo derivatives of $[XW_5O_{18}]^{3-}$ (X = Zr or Ti) have been investigated using density functional theory (DFT). The flexible bonding behavior of the linkage oxygen (O_L) atom attracted our attention initially, and NBO analysis revealed that there aret two different kinds of π-interactions involving the O_L atom in these systems. In two aryloxido derivatives (systems **1** and **2**), O_L–metal π-interactions are largely O_L–M p-d in character, whereas in the salicylaldehydo derivatives (system **3**) we observed another kind of π-interaction, namely O_L–C p-p π-bonding. The differences in molecular composition in our studied systems are very slight. However, the β_0 values differ significantly. Thus, system **3** has the largest β_0 value(559.27×10^{-30} esu), which is 170 times larger than that of system **1**. This variation can be traced to the different electronic transitions and charge-transfer characteristics. The heteropolyanion cluster and organic ligand are both electron-rich groups. A small change in molecular composition or architecture can therefore significantly modify the configuration and overlapping of molecular orbitals, thus causing a "butterfly effect" upon the electronic transitions and charge-transfer characteristics.

Introduction

Various classes of molecules have been explored for use as novel molecular NLO materials during the last few decades. These molecules can be grouped into three generic classes of NLO materials: inorganic salts, organic materials, and organometallic materials. Each class possesses its own complement of favorable and unfavorable attributes for NLO application.[1] Inorganic crystalline salts such as potassium dihydrogen phosphate (KH_2PO_4, KDP), for example, have already been widely used in commercial NLO devices,[2–4] although the NLO performance of such materials is not satisfactory. Recently, NLO studies of inorganic salts have become rare even though inorganic materials are robust and are available as large single crystals. The NLO responses of organic compounds often exceed those of purely inorganic substances,[5–7] although organic materials suffer several disadvantages which limit the applicability of such materials. For example, they usually have very poor thermal stability and (in poled host-guest systems) they may undergo a facile relaxation to a random orientation.[8] The limitations identified above have stimulated much research into the NLO properties of various alternative materials, among which organometallic complexes are of particular interest because of their potential for combining the advantages of both organic and inorganic materials.[9–16] The study of organometallic complexes with NLO properties has led to a number of important advances in this field, although the search for new molecular materials with large NLO response continues.

Recently, our attention has focused on polyoxometalate (POM)-based organic-inorganic hybrid materials.[17–20] POMs have been found to be extremely versatile inorganic building blocks for constructing functionally active materials, and POM-based organic-inorganic hybrid complexes are the combination of POM anions with organic or organometallic cations. There are several reasons why such materials are excellent candidates for novel NLO materials. Firstly, they offer a wide range of metals with different coordination states and various organic groups which possess large π-conjugated systems. Secondly, many of these compounds are known to possess intense low-lying electronic transitions. Finally, POMs have been found to be extremely flexible building blocks, which means non-centrosymmetric molecular structures can be relatively easily achieved for such compounds.

Since the pioneering work of Yan and co-workers,[17] who were the first to investigate the NLO properties of organoimido derivatives of hexamolybdates, much effort has

[a] Institute of Functional Material Chemistry, Faculty of Chemistry, Northeast Normal University,
Changchun 130024, P. R. China
Fax: +86-431-8568-4009
E-mail: zmsu@nenu.edu.cn

been directed towards a comprehensive understanding of the NLO properties of POM-based organic-inorganic materials.[18–20] However, the study of NLO properties of this class of materials remains in its infancy and understanding of their structure-property relationships is currently somewhat less substantial.

In this paper we report a theoretical study based on DFT and TD-DFT calculations of the bonding nature, first hyperpolarizabilities, electronic transitions, and charge-transfer characteristics involved in the nonlinear optical response of aryloxido and salicylaldehydo derivatives of $[XW_5O_{18}]^{3-}$ (X = Zr or Ti). These theoretical calculations were expected to achieve three goals: 1) to determine the bonding nature and interactions between the POM and organic ligand, 2) to predict the nonlinear optical properties and elucidate the structure-property relationships from the micromechanism, and 3) to provide useful guidelines for further studies of POM–ligand interactions involved in the NLO response.

Calculation Models

Errington and co-workers[21] recently reported the successful synthesis of a series of aryloxido and salicylaldehydo $[ZrW_5O_{18}]^{3-}$ derivatives. Since then a fairly large number of aryloxido derivatives $[TiW_5O_{18}]^{3-}$ have been synthesized.[22] The POM structures in these newly synthesized complexes are group 4 metal-substituted Lindqvist-type polytungstate anions $[XW_5O_{18}]^{3-}$ (X = Zr or Ti). The organic ligand is connected to the heteropolyanion cluster via linkage oxygen atoms (O_L). Three structures were chosen for the theoretical investigations reported herein (Figure 1). Systems **1** and **2** are aryloxido derivatives and their molecular composition is identical except for the heterometal (Zr and Ti in systems **1** and **2**, respectively). System **3** is a salicylaldehydo derivative. The salicylaldehydo ligand is able to bind in a chelating fashion and is connected to Zr via two linkage oxygen atoms − the phenolic oxygen (O_{L1}) and the aldehyde oxygen (O_{L2}). Although several aryloxido and salicylaldehydo derivatives have been synthesized, salicylaldehydo $[TiW_5O_{18}]^{3-}$ derivatives have not been successfully synthesized, therefore they were excluded from our calculations. In our previous studies[17,18] we systematically studied the bonding nature and NLO properties of organoimido and naphthylimido hexamolybdate derivatives. The results obtained from these previous studies are also discussed here as a reference.

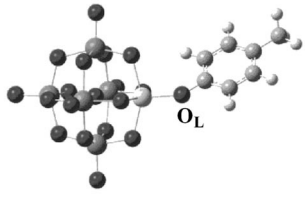

System 1 $[(4\text{-}MeC_6H_4O)ZrW_5O_{18}]^{3-}$ anion

System 2 $[(4\text{-}MeC_6H_4O)TiW_5O_{18}]^{3-}$ anion

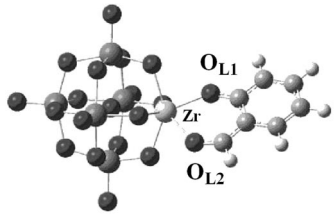

System 3 $[\{2\text{-}(CHO)C_6H_4O\}ZrW_5O_{18}]^{3-}$ anion

Figure 1. Structure of systems **1**–**3**.

Results and Discussion

Geometry

Geometry optimizations were performed without any symmetry constraints. The optimized partial geometrical parameters are listed in Table 1, which also includes experimental data.[21,22] Clearly, the important structural parameters are well-reproduced by the theoretical calculations. This suggests that our adopted method and basis sets are reliable for the systems studied. According to the literature, M–O bond lengths for group 4 metals are characterized by two features, namely that the M–O distances are very variable and are sometimes below the values expected on the basis of purely σ-bonding. These features were also observed in our studied systems. For example, an experimental study[23] has shown that a zirconium salicylaldehydo complex is characterized by an asymmetric "aryloxido and aldehydo" bonding mode. The Zr–O_{L1} bond (2.12 Å) in system **3** is shorter than the Zr–O_{L2} bond (2.28 Å). However, both these bonds are longer than the Zr–O_L bond (2.02 Å) in system **1**. In system **2**, the distance between Ti and O_L is shorter (1.85 Å) than the theoretical value for a single Ti–O covalent bond (2.01 Å).

Table 1. Selected average optimized bond lengths [Å] for systems **1**–**3**.

System	Atom pair	Bond length	
		Calculated	Experimental
1	Zr–O_L	2.02	2.03
	O_L–C	1.36	1.31
2	Ti–O_L	1.87	1.85
	O_L–C	1.36	1.31
3	Zr–O_{L1}	2.12	2.10
	Zr–O_{L2}	2.28	2.33
	O_{L1}–C	1.32	1.31
	O_{L2}–C	1.26	1.24

Natural Bond Orbital Analysis

Experimental studies[23–25] of early transition metal aryloxides have demonstrated the flexible nature of their bonding. To further investigate the bonding character, NBO analysis calculations were carried out on the basis of the optimized geometries. The results of these calculations are summarized in Tables 2 and 3. The presence of O_L-to-metal

Table 2. Bond type, occupancy, and orbital hybridization (orbital coefficients) for systems **1** and **2**.

System	Bond	Bond type	Occupancy	Orbital hybridization (orbital coefficients)
1	Zr=O_L	σ	1.9822	0.2633 $s^1d^{2.05}$(Zr) + 0.9647 $s^1p^{0.65}$(O)
		π	1.9253	0.2047 s^1 $p^{2.70}d^{16.55}$(Zr) + 0.9788 p^1(O)
	O_L –C	σ	1.9914	0.8143 $s^1p^{1.59}$(O) + 0.5805 s^1 $p^{2.94}$(C)
2	Ti=O_L	σ	1.9626	0.3271 s^1 $d^{1.83}$(Ti) + 0.9450 $s1p^{2.29}$(O)
		π	1.7917	0.2564 $s^1p^{1.54}d^{43.34}$(Ti) + 0.9666 P^1(O)
	O_L –C	σ	1.9900	0.8142 $s1p^{1.78}$(O) + 0.5806 $s1p^{2.65}$(C)

Table 3. Bond type, occupancy, and orbital hybridization (orbital coefficients) for system **3**.

Bond	Bond type	Occupancy	Orbital hybridization (orbital coefficients)
O_{L1}=C	σ	1.99148	0.8069$s^1p^{1.95}$(O) + 0.5906s^1 $p^{2.66}$(C)
	π	1.92740	0.8709 p^1(O) + 0.4914 p^1(C)
Zr–O_{L1}	σ	1.95290	0.2449$s^1p^{0.12}$ $d^{3.68}$(Zr) + 0.9696$s^1p^{2.17}$(O)
O_{L2}=C	σ	1.99438	0.8110 $s1p^{1.88}$(O) + 0.5850 $s1p^{2.39}$(C)
	π	1.95363	0.8246 p^1(O) + 0.5657 p^1(C)
Zr–O_{L2}	σ	1.94037	0.2273s^1p $0.^{05}d^{3.09}$(Zr) + 0.9738$s^1p^{3.67}$(O)

Table 4. Bond type, occupancy, and orbital hybridization (orbital coefficients) for arylimido hexamolybdates.

Bond	Bond type	Occupancy	orbital hybridization (orbital coefficients)
Mo≡N	σ	1.9772	0.4899 $s1p^{0.01}d^{4.64}$ (Mo) + 0.8718 $s^1p^{0.85}$ (N)
	π	1.8594	0.5619 d (Mo) + 0.8272 p (N)
	π	1.8403	0.5594 d(Mo) + 0.8289 p (N)
N–C	σ	1.9874	0.7670 $s^1p^{1.18}$ (N) + 0.6416 $s^1p^{2.51}$ (C)

p-d π-bonding has been proved in two aryloxido derivatives (system **1** and **2**) where a σ-bond and a p-d π-bond link O_L to the heterometal, which means that the interaction between the organic ligand and POMs in these two systems is similar to that in organoimido or naphthylimido hexamolybdate derivatives, where the Mo–N interactions suggest a triple bonding nature (Table 4).[26] The major difference is that there are two types of π-donation in the organoimido or naphthylimido hexamolybdate derivatives, namely donation from the occupied orbital of the arylimido into the empty d_{z^2} orbital of molybdenum and π back-donation from the d_{xz} and d_{yz} orbitals of molybdenum to the empty N p-orbital of the organoimido. There is only one type of π-interaction in systems **1** and **2**, namely O_L-to-metal π-donation.

Smith and co-workers,[25] who have systematically studied group 4 metal aryloxide derivatives, have reported that oxygen-p to metal-d π-donation is an important part of the bonding characteristics for d-block metals such as Ti and Zr and that the extent of π-bonding is very sensitive to the M–O bond length and the M–O–Ar bond angle. In our systems, this kind of π-interaction is only observed in two aryloxido derivatives. The NBO results show that both the Zr–O_L bonds in system **3** are σ single bonds, which clearly shows that there is a dramatic difference in the bonding of the aryloxide to the metal with respect to their salicylaldehydo counterparts. This is totally explicable if one recognizes that this kind of π-bonding is very sensitive to the M–O bond length and M–O–Ar bond angle. We suggest that these two structural parameters should be treated separately, as the M–O bond length determines the extent to which the oxygen-based p-orbital overlaps with the metal-based d-orbital, which can be used to estimate the degree of this kind of p-d π-bonding, and the M–O–Ar bond angle determines whether metal-based d-orbitals are available for bonding.

The NBO results also provide a rational interpretation why both the O_L–C bond lengths in system **3** are shorter than those in systems **1** and **2**. The results discussed above show that each of the two linkage O_L atoms in system **3** forms a p-p π-bond with its neighboring sp^2-hybridized carbon atom instead of forming the expected O_L-to-Zr p-d π-bond. Each of the two O_L=C bonds in the salicylaldehydo ligand shows double-bond character, which results in two shorter O_L=C bonds in system **3**. The ability to form O_L=C double bonds enables the p-electrons of the two O_L's to take part in the aromatic π-electron system, which extends the original benzene π-electron system to a nine-membered double ring aromatic π-system. In other words, system **3** possesses a larger organic π-conjugated system than the other systems studied.

Summary of NBO Analysis

The present investigation provides an important insight into POM–ligand interactions. NBO analysis of the flexible bonding behavior of the linkage O_L atom has revealed that there are two different kinds of π-interactions involving this atom in the systems studied. Thus, in aryloxide derivatives O_L–metal interactions are largely O-p–M-d in character and σ and π bonds link the O_L in the organic ligand to the heterometal in the POM. In system **3**, however, another kind of π-interaction, namely O_L–C p-p π-bonding, is pres-

ent. Interestingly, we have found that the relationship between these two kinds of π-interactions is competitive. The ability to form these two kinds of π-interactions is largely related to the p-donating ability of the linkage oxygen. In our case, the linkage oxygen is situated between the metal and the carbon atom, which compete with each other to interact with the p-electrons of this oxygen atom. Thus, if the p-d π-interaction between the metal atom and O_L is strong, then the p-p π-interaction between O_L and its neighboring carbon is weakened, and vice versa. This part of our work was inspired by the fact that understanding the nature of the bonding and intramolecular interactions in a system is a logical prerequisite for a rational interpretation of its structure-property relationships.

Orbital Character

One of the most striking features that can be observed from the molecular orbital diagrams is the extensive π-electron delocalization over the salicylaldehydo ligand, which involves participation of the p-electrons of two linkage oxygen atoms in system **3** (Figure 2). This feature corresponds to one of the conclusions obtained from the NBO analysis, namely that the ability of system **3** to form O_L=C double bonds enables the p-electrons of two O_L atoms to take part in the aromatic π-electron system, which extends the original benzene π-electron system to a nine-membered double ring aromatic π-system.

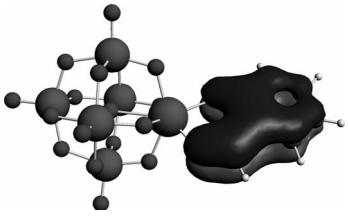

Figure 2. Diagram of the delocalized π-system in system **3**.

The frontier molecular orbital (FMO) diagrams for systems **1**–**3** are displayed in Figure 3, where the similarity between the FMOs of these systems can clearly be seen. For instance, the HOMO is delocalized over the oxo ligands and the molecular orbitals invoked in the LUMOs are π* orbitals delocalized over the organic ligands. These common features suggest that adding different ligands to the heteropolyanion cluster in these systems or introducing different heterometals (Zr or Ti) does not change the charge-transfer pattern, that is, the charge transfer originates from the heteropolyanion cluster to the organic ligand.

From our previous studies,[17,18] we found that the charge transfer in organoimido or naphthylimido hexamolybdate derivatives originates from the organic ligand to the $[Mo_6O_{18}]^{3-}$ cluster. It is interesting to note that the ground state POM–ligand interaction in these systems is the opposite of that in our studied systems.

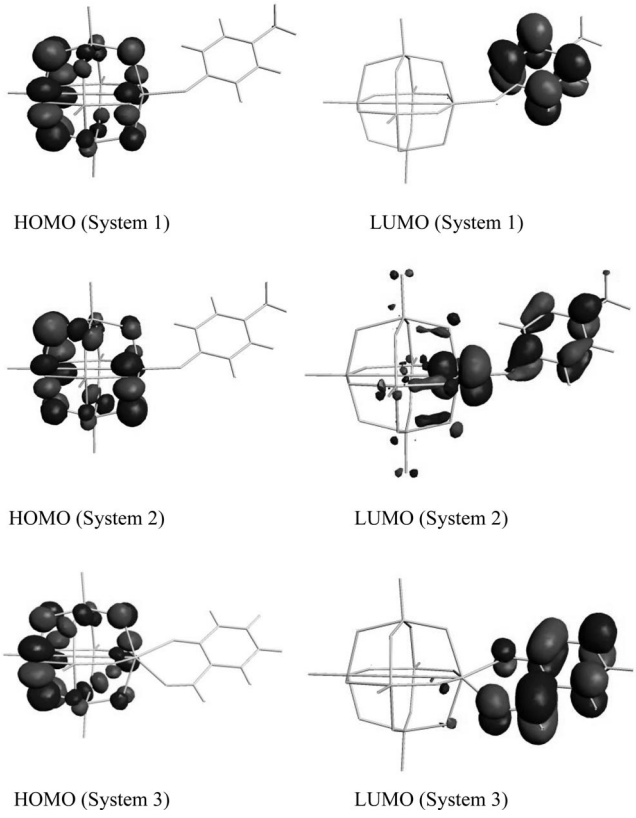

Figure 3. Frontier molecular orbitals of systems **1**–**3**.

Static First Hyperpolarizabilities

We also computed the static first hyperpolarizabilities (β_0) of systems **1**–**3**. The static first hyperpolarizability is an estimate of the intrinsic molecular first hyperpolarizability in the absence of any resonance effects. Thus, β_0 is defined as

$$\beta_0 = (\beta_x^2 + \beta_y^2 + \beta_z^2)^{1/2}$$

where $\beta_i = (3/5)\Sigma_j = {}_{x,y,z}\beta_{ijj}$.

The computed β_0 values for systems **1**–**3** are listed in Table 5, where it can be seen that system **1** has a moderate static second-order polarizability. The β_0 values for systems **2** and **3** are several times larger than those of typical organometallic complexes with extensive π-electron conjugation. System **3** has the largest β_0 value (170-times larger than that of system **1**), which means that the β_0 values differ significantly despite the fact that the differences in molecular composition are very slight.

Table 5. Computed first hyperpolarizabilities (β_0) and their individual components (1×10^{-30} esu) for systems **1**–**3**.

System	β_0	β_x	β_y	β_z	
1	3.30	0.216	3.30		–
2	19.19	16.20	10.30		–
3	559.27	6.272	2.30		599.22

What cause the variations in the computed β_0 values? To shed light on the origin of the second-order NLO performance of the studied systems it is necessary to elucidate the

structure-property relationships. Oudar and Chemla[27] have established a simple link between β_0 and electronic transition(s) in low-lying crucial excited states from the complex SOS expression. For the static case (ω = 0.0), the following two-level expression is employed to estimate β_0

$$\beta_0 = (3/2)\Delta\mu \times f_0/\Delta E^3$$

where ΔE, f_0, and μ are the transition energy, oscillator strength, and the difference in the dipole moment between the ground and the crucial excited state, respectively. In the two-level expression, the third power of the transition energy is inversely proportional to the β_0 value.

TD-DFT calculations were carried out to study the transition nature of systems **1**–**3**. The transition energies (ΔE) and oscillator strengths (f_0) of the crucial excited states are listed in Table 6, and the diagrams of related molecular orbitals are given in Figure 4.

The TD-DFT calculations reveal that the transition energies differ significantly for our studied systems. The transition energies of the two crucial electronic transitions of system **3** are only 0.468 and 1.246 eV, whereas they are 3.253 and 3.048 eV for systems **1** and **2**, respectively. As we discussed previously, the β_0 value is inversely proportional to the third power of ΔE, which means that even a small transition energy is a decisive factor and leads to a considerately large first hyperpolarizability of system **3**. This small transition energy is related to the electronic character rather than the geometric structure, The TD-DFT results show that two crucial excited states in system **3** dominate the optical nonlinearity. These two excited states are generated by promotion of the electron from HOMO-1 to the LUMO and HOMO-9 to the LUMO, respectively. As shown in Figure 4, the unoccupied molecular orbitals involved in these two crucial transitions are both the delocalized π* orbitals on the salicylaldehydo ligand. This highly delocalized π orbital accepts excited electrons from the heteropolyanion cluster and acts as an "excited electron" store. The charge transfer originates from the heteropolyanion cluster to the salicylaldehydo ligand mainly along the *z*-axis (the direction from the central oxygen to Zr is the *z*-axis in system **3**).

Table 6. Transition energy ΔE (eV), oscillator strength (f), and the corresponding crucial MO transitions for systems **1**–**3**.

System	ΔE	f	Major contribution
1	3.253	0.012	HOMO-1→LUMO + 6 (97.3%)
2	3.048	0.156	HOMO→LUMO + 5 (35.5%)
			HOMO-2→LUMO + 4 (19.6%)
3	0.468	0.121	HOMO-1→LUMO (88.3%)
	1.246	0.123	HOMO-9→LUMO (98%)

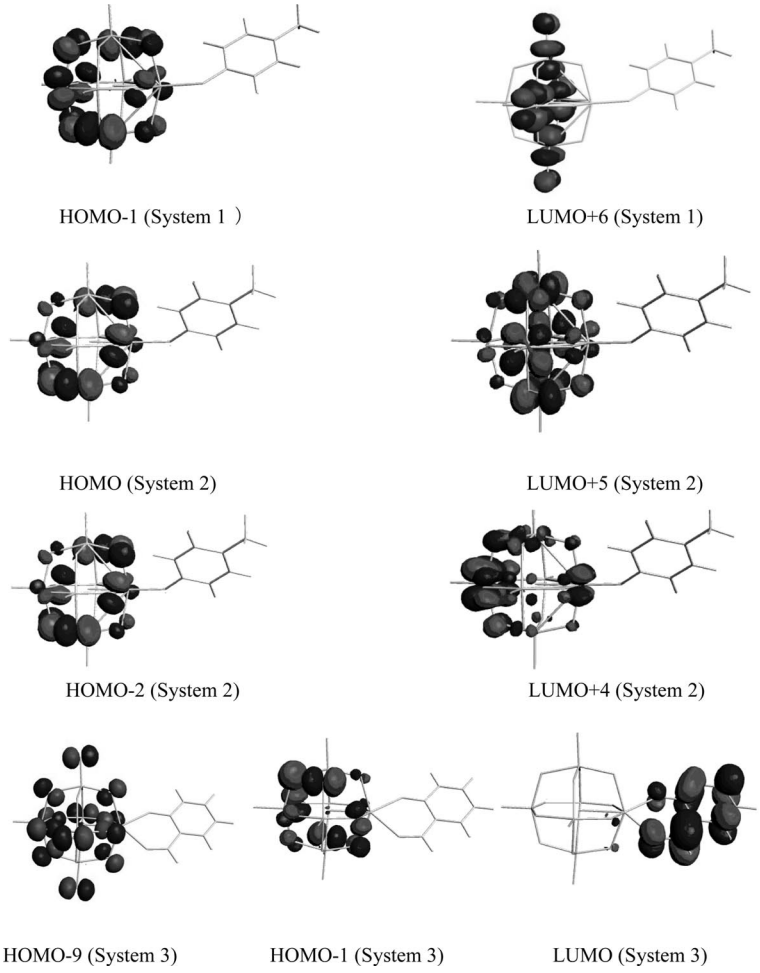

Figure 4. Molecular orbitals of systems **1**–**3** involved in the dominant electronic transition.

The molecular composition of systems **1** and **2** is identical except for the heteroatom. The symmetry of Lindqvist-type polytungstate anions $[W_6O_{19}]^{3-}$ is O_h, and it is well known that centrosymmetric structures show no second-order NLO response. When heteroatoms and an organic ligand are introduced, the symmetry is reduced to C_s, therefore the TD-DFT calculations on systems **1** and **2** were carried out under C_s symmetry (the *xy*-coordinate plane is defined as the reflection plane in these two systems).The TD-DFT analysis in terms of molecular orbitals shows that their crucial charge transfers follow a similar pattern, namely that the orbitals involved in the ground state are formally delocalized over the oxo ligands, and the unoccupied orbitals involved in the excited states are symmetry-adapted d-metal orbitals with some antibonding participation from O-p orbitals. The W–O interaction has W-d/O-p character. The main source of the crucial charge transfer(s) therefore appears to be the metal–oxygen interaction within the heteropolyanion cluster.

Conclusions

We have reported a theoretical study, based on DFT and TD-DFT calculations, of the bonding nature, first hyperpolarizabilities, electronic transitions, and charge transfer involved in the nonlinear optical response of aryloxido and salicylaldehydo derivatives of $[XW_5O_{18}]^{3-}$ (X = Zr or Ti). Geometry optimizations, performed without any symmetry constraints, have confirmed the asymmetric "aryloxido and aldehyde" bonding mode in salicylaldehydo $[ZrW_5O_{18}]^{3-}$ derivatives, and NBO analysis has revealed that there are two different kinds of π-interactions involving the linkage O_L atom in our studied systems. Thus, in the two aryloxido derivatives (systems **1** and **2**) O_L–metal interactions are largely O-p/M-d in character and σ and π bonds link the O_L in the organic ligand to the heterometal in the heteropolyanion cluster. In salicylaldehydo derivatives (system **3**), however, both the Zr–O_L bonds are σ single bonds. Each of the two linkage O_L atoms is involved in p-p π-bonding with a neighboring sp^2-hybridized carbon in the organic ligand instead of forming the expected O_L-to-Zr p-d π-bond. The computational results therefore provide a rational interpretation of several problems that could not be resolved experimentally.

The differences in molecular composition in our studied systems are very slight, whereas the β_0 values differ significantly. Thus, system **3** possesses a remarkably large molecular static first hyperpolarizability (559.271×10^{-30}), which is about 170 times higher that of system **1**. This variation can be traced to the different electronic transition and charge-transfer characteristics. The TD-DFT molecular orbital analysis indicates that the low-lying charge transfer from the heteropolyanion cluster to the organic ligand in system **3** is responsible for this remarkably large molecular static first hyperpolarizability. In systems **1** and **2**, however, the main origin of the crucial charge transfer(s) is the metal–oxygen interaction within the heteropolyanion cluster. It is interesting to note that the differences in NLO response between salicylaldehydo and aryloxido derivatives is not just a matter of degree but also of kind. This due to the fact that the heteropolyanion cluster and organic ligand are both electron-rich groups, which means that a small change in molecular composition or POM–ligand interactions will cause a "butterfly effect" upon the electronic transition and charge-transfer characteristics. We are now in a position to study this mechanism in detail, although further studies are still necessary to establish a universal theoretical mode for POM–ligand interactions involved in NLO response.

Guideline for Further Studies and Molecular Design

The two-level model has been used to rationalize the NLO response of conventional compounds. Our results, together with our previous studies,[17–20] have proved the effectiveness of this model in rationalizing the NLO response of large and electron-rich systems. We therefore believe that the guidelines in this section should be based on this model. Previously studied POM-based organic-inorganic hybrid systems usually contain two kinds of major charge transfers, namely the charge transfer within the POM cluster and the charge transfer between the POM cluster and the organic ligand. The latter can trigger a significant change in dipole moment, which is crucial in boosting the NLO response of systems. In cases where the charge transfer originates from the POM cluster to the organic ligand, systems with a large NLO response usually possess one or several low-lying organic π (or π*) orbitals. In cases where the charge transfer originates from the organic ligand to the POM cluster, however, systems with a large NLO response usually possess several low-lying metal-based d orbitals. These two kinds of orbitals are found to be frequently involved in the crucial electronic-transition processes. Additionally, we suggest that more attention should be paid to the organic ligating groups and the metals to which these organic ligands are attached. The latter often engage in π-bonding with both organic ligating groups and with atoms in the POM cluster. The organic ligating groups often participate in low-energy π electronic transition processes, which have been found to be associated with a large NLO response in both purely organic and organometallic systems.

Methodology

In all calculations except for NBO analysis calculations, the DFT calculations were carried out using the ADF2006.01 program.[28,29] The geometries of all systems were optimized and the initial geometric data were obtained from the crystal data.[21,22] The local density approximation (LDA) characterized by the Vosko-Wilk-Nusair (VWN)[30] parametrization for correlation was used. The generalized-gradient approximation (GGA) was employed in the geometry optimizations by using the Beck[30,31] and Perdew[32] exchange-correlation (XC) functional. The zero-order regular approximation (ZORA) was adopted in all calculations to account for scalar relativistic effects.[33] The basis functions were Slater-type

sets. Triple-ζ plus polarization basis sets were used to describe the valence electrons of all atoms, whereas core orbitals were frozen as follows: 1s (C, N, O), 3p (Ti), 3d (Zr), 4d (W). In calculations of the, hyperpolarizability and excitation properties, the RESPONSE and EXCITATION modules[34] implemented in the ADF program were used on the basis of the optimized geometries. The van Leeuwen-Baerends XC potential[35] (LB94) was chosen for calculations of all the response properties.

To further ascertain the bonding characters of our studied systems we performed single-point natural bond orbital analysis calculations on the basis of the optimized geometries, using the Gaussian98 program at the B3LYP level. In all Gaussian98 calculations the LANL2DZ basis set associated with the pseudopotential was used to describe the W atoms and the 6-31G(d) basis set was used to describe the C, O and H atoms. The SDD basis set, which takes into account relativistic effects, was used for Zr and Ti due to its accuracy in describing early transition metals.

Acknowledgments

The authors gratefully acknowledge financial support from the National Natural Science Foundation of China (project nos. 20373009 and 20703008), the Chang Jiang Scholars Program (2006), the Program for Chang Jiang Scholars and Innovative Research Team in University (IRT0714), the National High-Tech Research and Development Program (863 Program 2007AA03Z354), the Science Foundation for Young Teachers of NENU (20070304 and 20070309), and the Training Fund of NENU's Scientific Innovation Project (NENU-STC07017).

[1] W. Blau, *Phys. Technol.* **1987**, *18*, 250–268.
[2] P. Harper, B. Wherrett, *Nonlinear Optics*, Academic Press, New York, **1977**.
[3] Y. R. Shen, *The Principles of Nonlinear Optics*, Wiley, New York, **1984**.
[4] B. E. A. Saleh, M. C. Teich, *Fundamentals of Photonics*, Wiley, New York, **1991**.
[5] D. S. Chemla, J. Zyss, *Nonlinear Optical Properties of Organic Molecules and Crystals*, Academic Press: Orlando, FL, **1987**, Vols. 1 and 2.
[6] J. Zyss, *Molecular Nonlinear Optics: Materials, Physics and Devices*, Academic Press: Boston **1994**.
[7] H. S. Nalwa, S. Miyata, *Nonlinear Optics of Organic Molecules and Polymers*, CRC Press: Boca Raton, FL, **1997**.
[8] C. E. Powell, M. G. Humphrey, *Coord. Chem. Rev.* **2004**, *248*, 725–756.
[9] H. S. Nalwa, *Appl. Organomet. Chem.* **1991**, *5*, 349–377.
[10] N. Long, *Angew. Chem. Int. Ed. Engl.* **1995**, *34*, 21–38.
[11] I. R. Whittall, A. M. McDonagh, M. G. Humphrey, M. Samoc, *Adv. Organomet. Chem.* **1998**, *42*, 291–361.
[12] J. Qin, D. Liu, C. Dai, C. Chen, B. Wu, C. Yang, C. Zhan, *Coord. Chem. Rev.* **1999**, *188*, 23–34.
[13] J. Heck, S. Dabek, T. Meyer-Friedrichsen, H. Wong, *Coord. Chem. Rev.* **1999**, *190–192*, 1217–1254.
[14] H. Le Bozec, T. Renouard, *Eur. J. Inorg. Chem.* **2000**, 229–239.
[15] S. Barlow, S. R. Marder, *Chem. Commun.* **2000**, 1555–1562.
[16] S. Di Bella, *Chem. Soc. Rev.* **2001**, *30*, 355–366.
[17] L. K. Yan, G. C. Yang, W. Guang, Z. M. Su, R. S. Wang, *J. Phys. Chem. B* **2005**, *109*, 22332–22336.
[18] L. K. Yan, M. S. Jin, J. Zhuang, C. G. Liu, Z. M. Su, C. C. Sun, *J. Phys. Chem. A* **2008**, *112*, 9919–9923.
[19] W. Guang, G. C. Yang, L. K. Yan, Z. M. Su, *Inorg. Chem.* **2006**, *45*,7864–7868.
[20] G. C. Yang, W. Guang, L. K. Yan, Z. M. Su, *J. Phys. Chem. B* **2006**, *110*, 23092–23098.
[21] R. J. Errington, S. S. Petkar, P. S. Middleton, W. McFarlane, W. Clegg, R. A. Coxall, R. W. Harrington, *J. Am. Chem. Soc.* **2007**, *129*, 12181–12196.
[22] R. J. Errington, S. S. Petkar, P. S. Middleton, W. McFarlane, W. Clegg, R. A. Coxall, R. W. Harrington, *Dalton Trans.* **2007**, 5211–5222.
[23] L. Matilainen, M. Klinga, M. Leskela, *J. Chem. Soc., Dalton Trans.* **1996**, 219–225.
[24] a) D. C. Bradley, R. C. Mehrotra, D. P. Gaur, *Metal Alkoxides*, Academic Press, London, UK, **1978**; b) D. C. Bradley, R. C. Mehrotra, I. P. Rothwell, A. Singh, *Alkoxo and Aryloxo Derivatives of Metals* Academic Press, London, UK, **2001**.
[25] G. D. Smith, P. E. Fanwick, I. P. Rothwell, *Inorg. Chem.* **1990**, *29*, 3221–3226.
[26] L. K. Yan, Z. M. Su, W. Guan, M. Zhang, G. H. Chen, L. Xu, E. B. Wang, *J. Phys. Chem. B* **2004**, *108*, 17337–17342.
[27] a) J. L. Oudar, D. S. Chemla, *J. Chem. Phys.* **1977**, *66*, 2664–2668; b) J. L. Oudar, *J. Chem. Phys.* **1977**, *67*, 446–457.
[28] a) G. te Velde, F. M. Bickelhaupt, S. J. A. van Gisbergen, C. Fonseca Guerra, E. J. Baerends, J. G. Snijders, T. Ziegler, *J. Comput. Chem.* **2001**, *22*, 931; b) C. Fonseca Guerra, J. G. Snijders, G. te Velde, E. Baerends, *J. Theor. Chem. Acc.* **1998**, *99*, 391–403.
[29] ADF **2002**, 03, SCM, Theoretical Chemistry; Vrije Universiteit, Amsterdam, The Netherlands.
[30] S. H. Vosko, L. Nusair, M. Can, *J. Phys. (Paris)* **1980**, *58*, 1200–1211.
[31] A. D. Becke, *Phys. Rev. A* **1988**, *38*, 3098–3100.
[32] J. P. Perdew, *Phys. Rev. B* **1986**, *33*, 8822–8824.
[33] E. van Lenthe, E. J. Baerends, J. G. Snijders, *J. Chem. Phys.* **1993**, *99*, 4597–4610.
[34] S. J. A. van Gisbergen, J. G. Snijders, E. Baerends, *Comput. Phys. Commun.* **1999**, *118*, 119–138.
[35] R. van Leeuwen, E. Baerends, *J. Phys. Rev.* **1994**, *49*, 2421–2431.

Received: January 6, 2009
Published Online: April 29, 2009

